


Cite this: *RSC Adv.*, 2023, **13**, 6124

Received 31st January 2023  
Accepted 15th February 2023

DOI: 10.1039/d3ra00665d  
rsc.li/rsc-advances

## Spirocitrinols A and B, citrinin derivatives with a spiro[chromane-2,3'-isochromane] skeleton from *Penicillium citrinum*†

Junjie Tong,‡<sup>ab</sup> Yang Zhang, ‡<sup>c</sup> Yang Xu, <sup>b</sup> Yangyang Han, <sup>b</sup> Chuan Li, \*<sup>b</sup> Wenying Zhuang<sup>d</sup> and Yongsheng Che\*<sup>ab</sup>

Spirocitrinols A (**1**) and B (**2**), two new citrinin-derived metabolites possessing a spiro[chromane-2,3'-isochromane] skeleton, were isolated from cultures of *Penicillium citrinum*. Their structures were elucidated primarily by NMR experiments. The absolute configurations of **1** and **2** were assigned by electronic circular dichroism calculations. Compound **2** is the first naturally occurring trimeric citrinin derivative with a spiro[chromane-2,3'-isochromane] core. Compound **1** showed modest cytotoxicity against A549 human tumor cells.

## Introduction

Citrinin is a typical polyketide mycotoxin first discovered from a *Penicillium citrinum* strain in 1931.<sup>1</sup> Citrinin derivatives could be dimerized or trimerized to form highly complex polycyclic natural products with a variety of biological activities.<sup>2,3</sup> This class of natural products are encountered as the secondary metabolites of fungi, especially among species of *Penicillium* sp. and *Monascus* sp. but also sporadically in *Aspergillus* sp. from both terrestrial and marine environments.<sup>4</sup>

Benzannulated spiroketals are privileged scaffolds commonly encountered in natural products and drugs with the benzannulated 5,5-, 6,5-, and 6,6-spiroketal cores.<sup>5</sup> While naturally occurring bisbenzannulated 6,6-spiroketals are categorized into two type of skeletons (Fig. 1), 2,2'-spirobi[chromane] and spiro[chromane-2,3'-isochromane]. To our knowledge, only a few precedents with a spiro[chromane-2,3'-isochromane] core have been reported as dimeric citrinin derivatives to date,<sup>6,7</sup> two of which are xerucitrin acids A and B.

isolated from the fungus *Xerula* sp. BCC56836,<sup>6</sup> and xerucitrinins A–C identified from *Penicillium citrinum*.<sup>7</sup>

*Penicillium citrinum* has attracted much attention due to frequent discovery of structurally diverse and biologically active natural products from this fungal species.<sup>8</sup> In efforts to identify new cytotoxic metabolites from the fungi of various habitats,<sup>9</sup> a strain of *P. citrinum* isolated from a soil sample collected from the Yongxing Island, Hainan province, People's Republic of China, was subjected to a chemical investigation. Fractionation of an EtOAc extract prepared from the solid-substrate fermentation cultures led to the isolation of spirocitrinols A (**1**, Fig. 2) and B (**2**), two new citrinin-derived metabolites possessing a rare spiro[chromane-2,3'-isochromane] skeleton. Details of



Fig. 1 Two types of skeletons in naturally occurring bisbenzannulated 6,6-spiroketals.

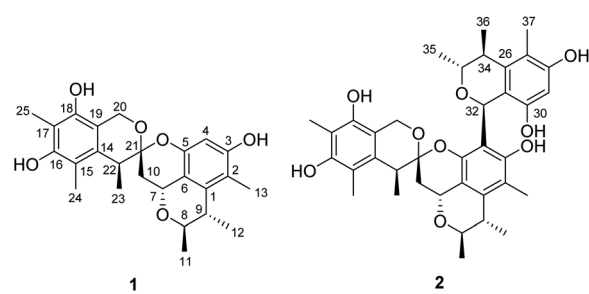


Fig. 2 Structures of compounds **1** and **2**.

<sup>a</sup>Tianjin University of Traditional Chinese Medicine, Tianjin, 300193, People's Republic of China

<sup>b</sup>NHC Key Laboratory of Biotechnology of Antibiotics, Institute of Medicinal Biotechnology, Chinese Academy of Medical Sciences & Peking Union Medical College, Beijing, 100050, People's Republic of China. E-mail: ysche@imb.cams.cn; licuan@imb.cams.cn

<sup>c</sup>State Key Laboratory of Toxicology & Medical Countermeasures, Beijing Institute of Pharmacology & Toxicology, Beijing, 100850, People's Republic of China

<sup>d</sup>State Key Laboratory of Mycology, Institute of Microbiology, Chinese Academy of Sciences, Beijing, 100101, People's Republic of China

† Electronic supplementary information (ESI) available: HRESIMS, NMR spectra, and ECD calculations of compounds **1** and **2**. See DOI: <https://doi.org/10.1039/d3ra00665d>

‡ These authors contributed equally to this work.



the structure elucidation, cytotoxicity evaluation, and plausible biogenesis of **1** and **2** are reported herein.

## Results and discussion

Spirocitrinol A (**1**) had a molecular formula of  $C_{25}H_{30}O_6$  (11 degrees of unsaturation) as deduced from its HRESIMS and the NMR spectroscopic data (Table 1). Analysis of its NMR data revealed the presence of three exchangeable protons ( $\delta_H$  9.05, 7.83, and 7.88, respectively), six methyl groups, two methylene units (one oxygenated), four methines (two oxygenated), one

Table 1 NMR data of **1** and **2**

	<b>1</b>		<b>2</b>	
No.	$\delta_C$ <sup>a</sup> , type	$\delta_H$ <sup>b</sup> ( $\delta$ in Hz)	$\delta_C$ <sup>a</sup> , type	$\delta_H$ <sup>b</sup> ( $\delta$ in Hz)
1	136.5, qC		134.0, qC	
2	114.5, qC		113.8, qC	
3	155.6, qC		153.1, qC	
4	99.9, qC	5.91, s	113.8, qC	
5	149.2, qC		147.6, qC	
6	110.7, qC		112.7, qC	
7	59.3, CH	4.77, dd (4.2, 12.0)	60.4, CH	4.72, brd (12.0)
8	74.2, CH	4.02, m	74.2, CH	4.02, m
9	34.6, CH	2.62, m	34.3, CH	2.58, m
10a	35.9, CH <sub>2</sub>	2.31, dd (4.8, 12.0)	38.2, CH <sub>2</sub>	2.38, dd (4.2, 12.0)
10b		1.68, t (12.0)		1.61, t (12.0)
11	18.7, CH <sub>3</sub>	1.28, d (6.6)	18.5, CH <sub>3</sub>	1.28, d (6.6)
12	22.7, CH <sub>3</sub>	1.11, d (7.2)	22.5, CH <sub>3</sub>	1.12, d (6.6)
13	10.5, CH <sub>3</sub>	1.94, s	10.3, CH <sub>3</sub>	1.85, s
14	133.6, qC		133.8, qC	
15	113.7, qC		113.3, qC	
16	152.6, qC		152.0, qC	
17	110.6, qC		110.0, qC	
18	148.3, qC		148.3, qC	
19	111.9, qC		111.7, qC	
20a	60.8, CH <sub>2</sub>	4.45, d (15.0)	61.3, CH <sub>2</sub>	4.71, d (14.4)
20b		4.71, d (15.0)		4.77, d (13.8)
21	101.2, qC		101.4, qC	
22	38.0, CH	2.85, brd (7.2)	38.6, CH	2.92, t (6.6)
23	18.6, CH <sub>3</sub>	1.05, d (6.6)	17.9, CH <sub>3</sub>	1.07, d (6.6)
24	11.0, CH <sub>3</sub>	2.01, s	10.6, CH <sub>3</sub>	1.89, s
25	9.9, CH <sub>3</sub>	2.04, s	9.7, CH <sub>3</sub>	1.95, s
26			138.5, qC	
27			112.9, qC	
28			155.4, qC	
29			100.8, CH	6.11, s
30			152.3, qC	
31			111.5, qC	
32			61.9, CH	5.45, s
33			73.0, CH	3.67, m
34			35.0, CH	2.40, m
35			16.1, CH <sub>3</sub>	0.50, d (6.6)
36			20.3, CH <sub>3</sub>	1.21, d (6.6)
37			10.4, CH <sub>3</sub>	1.92, s
3-OH		9.05, s		5.90, s
16-OH		7.83, s		7.59 <sup>c</sup> , s
18-OH		7.88, s		7.80 <sup>c</sup> , s
28-OH				8.99 <sup>c</sup> , s
30-OH				8.75, s

<sup>a</sup> Recorded in DMSO-*d*<sub>6</sub> at 150 MHz. <sup>b</sup> Recorded in DMSO-*d*<sub>6</sub> at 600 MHz. <sup>c</sup> These assignments are interchangeable.

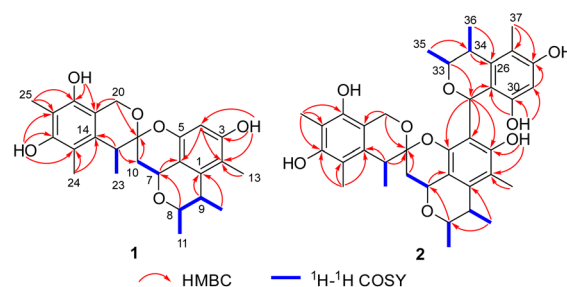


Fig. 3 Key  $^1H$ - $^1H$  COSY and HMBC correlations of **1** and **2**.

doubly oxygenated sp<sup>3</sup> quaternary carbon ( $\delta_C$  101.2), and 12 aromatic carbons with one protonated. These data accounted for all of the NMR resonances, suggesting that **1** was a pentacyclic compound. The  $^1H$ - $^1H$  COSY NMR data of **1** (Fig. 3) showed three isolated spin-systems, which were C-7–C-10, C-11–C-8–C-9–C-12, and C-22–C-23. The HMBC correlations from H-4 to C-2, C-3, C-5, and C-6, H-7 to C-1 and C-6, H-8 to C-7, and from H-9 to C-1 established an isochromane moiety, which was partially supported by the downfield chemical shifts of C-7 ( $\delta_C$  59.3) and C-8 ( $\delta_C$  74.2). The H<sub>3</sub>-11, H<sub>3</sub>-12, and H<sub>3</sub>-13 methyl groups were located at C-8, C-9, and C-2, respectively, by relevant HMBC cross peaks. While the exchangeable proton at 9.05 ppm was assigned to the free hydroxy group attached to C-3 based on the HMBC correlations from this proton (OH-3) to C-2, C-3, and C-4. Further correlations from H-7 to C-10 and C-21 led to the connection of C-10 to C-21, and those of H<sub>2</sub>-10 and H-22 with the doubly oxygenated tertiary carbon at 101.2 ppm enabled connection of C-21 to C-10 and C-22. In turn, the HMBC correlations from H<sub>2</sub>-20 and H-22 to C-14 and C-19, H<sub>3</sub>-24 to C-14, C-15, and C-16, and from H<sub>3</sub>-25 to C-16, C-17, and C-18 established the second polysubstituted aryl ring in **1**. The remaining two exchangeable protons at 7.83 and 7.88 ppm were assigned to the free hydroxy groups located at C-16 and C-18, respectively, on the basis of relevant HMBC correlations. HMBC correlation from H<sub>2</sub>-10 to C-21 revealed the presence of the second isochromane unit in **1**. Considering the unsaturation requirement of **1**, the doubly oxygenated nature of C-21 ( $\delta_C$  101.2), and the chemical shift values for C-5 ( $\delta_C$  149.2) and C-20 ( $\delta_C$  60.8), the two C-21 bonded oxygen atoms were individually attached to C-5 and C-20 by default to complete the gross structure of **1** as shown. Compound **1** was found to be a stereoisomer of the known fungal metabolite xerucitrinol A,<sup>7</sup> when comparison of its NMR data acquired in deuterated MeOH (Table S1†) with those of the known precedent.

The relative configuration of **1** was deduced by analysis of the  $^1H$ - $^1H$  coupling constants and NOESY data (Fig. 4). A coupling constant of 4.8 Hz observed between H-10a and H-7 suggested their *cis* relationship.<sup>6</sup> The NOESY cross peaks of H<sub>3</sub>-11 with H-7 and H-9, and of H-10a with H-7 and H<sub>3</sub>-23 placed these protons on the same face of 3,3a,5,6-tetrahydro-2*H*-pyrano[2,3,4-*de*]chromene moiety, whereas the correlations of H-10b and H-22, and of H-8 with H<sub>3</sub>-12 revealed their spatial proximity, and suggested that they were on the opposite face of the ring system. On the basis of these data, the relative configuration of **1** was



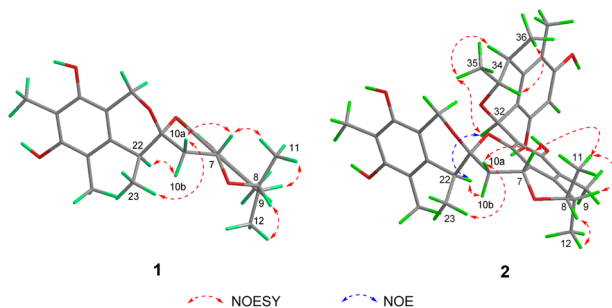


Fig. 4 Key NOESY correlations of **1** and **2** and NOE correlation of **2**.

proposed as shown. The absolute configuration of **1** was deduced by comparison of the experimental and simulated electronic circular dichroism (ECD) spectra generated by time-dependent density functional theory (TDDFT), for enantiomers *7R,8R,9S,21R,22S*-**1** (**1a**) and *7S,8S,9R,21S,22R*-**1** (**1b**).<sup>10</sup> The MMFF94 conformational search followed by reoptimization using TDDFT at the B3LYP/6-31G(d) basis set level afforded the lowest-energy conformers for **1a** (Fig. S14†). The overall calculated ECD spectra of **1a** was then generated by Boltzmann weighting of their lowest-energy conformers by their relative free energies. The absolute configuration of **1** was then extrapolated by comparison of the experimental and calculated ECD spectra of **1a** and **1b** (Fig. 5). The experimental ECD spectrum of **1** was nearly identical to the calculated ECD curve of *7R,8R,9S,21R,22S*-**1** (**1a**), both showing two negative Cotton effects (CEs) in the ranges of 210–250 and 250–300 nm, respectively, suggesting that **1** has the *7R,8R,9S,21R,22S* absolute configuration.

Spirocitrinol B (**2**) was determined to have a molecular formula of  $C_{37}H_{44}O_9$  (16 degrees of unsaturation) based on

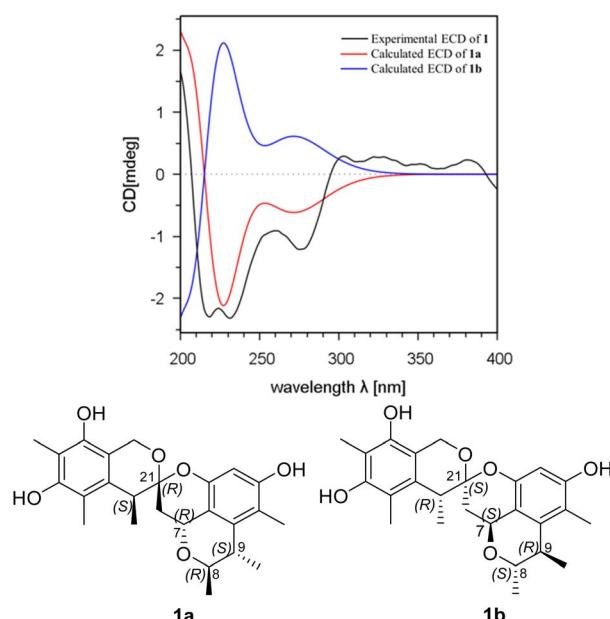


Fig. 5 Experimental ECD spectrum of **1** in MeOH and the calculated ECD spectra of **1a** and **1b**.

HRESIMS and NMR data (Table 1). Comparison of  $^1H$  and  $^{13}C$  NMR data with those of **1** indicated that there was a 4-substituted-1 substructure in **2**. The remaining resonances for **2** indicated the presence of a known citrinin derivative, decarboxydihydrocitrinin,<sup>2a</sup> which was confirmed by interpretation of the 2D NMR data. The HMBC correlations from H-29 to C-27, C-28 and C-30, from H-32 to C-26 and C-31, from H-33 to C-32, and from H-34 to C-26 and C-31, plus the downfield chemical shifts of C-32 ( $\delta_C$  61.9) and C-33 ( $\delta_C$  73.0), established the third isochromane unit in **2**. The  $H_{3\cdots}35$ ,  $H_{3\cdots}36$ , and  $H_{3\cdots}37$  methyl groups were located at C-33, C-34, and C-27, respectively, by relevant HMBC cross peaks. The exchangeable proton at 8.75 ppm was assigned to the free hydroxy group attached to C-30 based on the HMBC correlations from this proton (OH-30) to C-29, C-30, and C-31. Considering the chemical shift of C-28 ( $\delta_C$  155.4) and by comparison to the similar chemical shift of C-3 ( $\delta_C$  155.6) in **1**, another free hydroxy group is required to attach to C-28, although no additional evidence was provided by the HMBC data. In addition, the HMBC correlations from H-32 to C-3, C-4, and C-5, established the C-4–C-32 linkage between the two units. Collectively, the planar structure of a novel trimeric citrinin derivative for **2** was tentatively assigned as shown. The relative configuration of the 4-substituted-1 substructure in **2** was determined to be the same as that of **1** by analysis of its coupling constant and NOESY data. The NOESY correlations of  $H_{3\cdots}35$  with  $H_{3\cdots}32$  and  $H_{3\cdots}34$  indicated that these protons adopt the same orientation for the remaining 3,4,5-trimethylisochromane-6,8-diol unit. In addition, NOE correlation of H-22 with H-32 revealed their proximity in space, thereby allowing deduction of the relative configuration for **2**. The absolute configuration of **2** was proposed by comparison of the

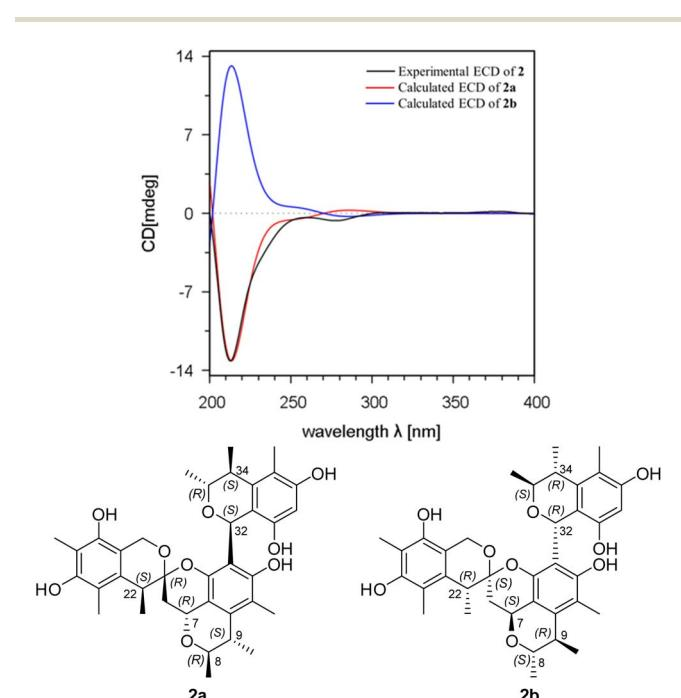


Fig. 6 Experimental ECD spectrum of **2** in MeOH and the calculated ECD spectra of **2a** and **2b**.



Table 2 Cytotoxicity of compounds 1 and 2

Compounds	IC <sub>50</sub> <sup>a</sup> (μM)						
	SKBR3	HepG2	A549	J82	MB49 (STR)	Huh7	MB49 (WT)
1	49.2 ± 3.3	41.6 ± 8.1	4.3 ± 0.4	45.6 ± 2.5	49.3 ± 7.8	48.2 ± 5.6	43.3 ± 4.5
2	48.1 ± 6.5	41.2 ± 6.3	11.8 ± 2.8	48.7 ± 2.8	55.7 ± 10.8	44.1 ± 7.9	64.5 ± 6.7
Cisplatin <sup>b</sup>	3.6 ± 0.6	4.8 ± 0.9	6.5 ± 1.0	0.61 ± 0.1	9.6 ± 1.9	5.1 ± 1.6	5.1 ± 1.6

<sup>a</sup> IC<sub>50</sub> values were averaged from at least three independent experiments. <sup>b</sup> Positive control.

experimental and calculated ECD spectra generated for enantiomers **2a** and **2b** (Fig. 6). MMFF94 conformational search followed by B3LYP/6-31G(d)DFT reoptimization afforded lowest-energy conformers (Fig. S15†). The calculated ECD spectra of **2a** and **2b** were then generated by Boltzmann weighting of their lowest-energy conformers. The experimental ECD spectrum of **2** matches the calculated ECD curve of **2a** but is opposite to that of **2b**, suggesting the *7R,8R,9S,21R,22S,32S,33R,34S* configuration.

*In vitro* cytotoxic activity of compounds **1** and **2** was evaluated against seven tumor cell lines including SKBR3 (human breast cancer), HepG2 (human hepatoma), A549 (human lung cancer), J82 (human bladder carcinoma), MB49 (STR) (cisplatin resistant mouse bladder cancer), Huh7 (human hepatoma) cell lines, and MB49 (WT) (cisplatin sensitive mouse bladder cancer) (Table 2). Compound **1** showed modest cytotoxicity against A549 cells, with IC<sub>50</sub> value of 4.3 ± 0.4 μM, compound **2** was cytotoxic to A549 cells, with IC<sub>50</sub> value of 11.8 ± 2.8 μM, while the positive control cisplatin showed IC<sub>50</sub> of 6.5 ± 1.0 μM.<sup>11,12</sup>

## Experimental

### General experimental procedures

The culture of *Penicillium citrinum* was isolated from a soil sample that was collected in Yongxing Island, Hainan province, People's Republic of China, in November 2016. The isolate was identified based on morphology and sequence (Genbank Accession No. ON307318) analysis of the ITS region of the rDNA. The strain was cultured on slants of potato dextrose agar at 25 °C for 10 days. Agar plugs were cut into small pieces (about 0.5 × 0.5 × 0.5 cm<sup>3</sup>) under aseptic conditions, and 25 pieces were used to inoculate in five 250 mL Erlenmeyer flasks, each containing 50 mL of media (0.4% glucose, 1% malt extract, and 0.4% yeast extract; pH adjusted to 6.5 and sterilized by autoclave). Five flasks of the inoculated media were incubated at 25 °C on a rotary shaker at 170 rpm for 5 days to prepare the seed culture. Fermentation was carried out in 20 Fernbach flasks (500 mL), each containing 80 g of rice. Distilled H<sub>2</sub>O (120 mL) was added to each flask, and the contents were soaked overnight before autoclaving at 15 psi for 30 min. After cooling to room temperature, each flask was inoculated with 5.0 mL of the spore inoculum and incubated at 25 °C for 40 days.

### Extraction and isolation

The fermentation material was extracted repeatedly with EtOAc (2 × 3.0 L), and the organic solvent was evaporated to dryness

under vacuum to afford 5.2 g of extract. The extract was fractionated by silica gel vacuum liquid chromatography (VLC) using petroleum ether-EtOAc-MeOH gradient elution. The fraction (80.2 mg) eluted with 100 : 30 petroleum ether-EtOAc was subjected to Sephadex LH-20 column chromatography (CC) eluting with 1 : 1 CH<sub>2</sub>Cl<sub>2</sub>-MeOH and the resulting subfractions were combined and purified using semipreparative HPLC (45% MeCN in H<sub>2</sub>O, Agilent Zorbax SB-C18 column; 5 μm; 9.4 × 250 mm, 3 mL min<sup>-1</sup>) to give **1** (12.3 mg, t<sub>R</sub> 18.2 min), the resulting subfractions were combined and purified using semipreparative HPLC (50% MeCN in H<sub>2</sub>O, Agilent Zorbax SB-C18 column; 5 μm; 9.4 × 250 mm, 3 mL min<sup>-1</sup>) to give **2** (4.0 mg, t<sub>R</sub> 30.0 min).

**Spirocitrinol A (1):** colorless oil; [α]<sup>25</sup><sub>D</sub> +18.0 (c 0.1, MeOH); UV (MeOH)  $\lambda_{\text{max}}$  (log ε) 204 (0.88), 284 (0.03); IR (KBr)  $\nu_{\text{max}}$  3412, 2922, 1631, 1105, 908 cm<sup>-1</sup>; ECD (c 2.0 × 10<sup>-5</sup> M, MeOH)  $\lambda_{\text{max}}$  (Δε) 231 (-2.30), 275 (-1.21) nm; <sup>1</sup>H and <sup>13</sup>C NMR data see Table 1; HMBC data (DMSO-*d*<sub>6</sub>, 600 MHz) H-4 → C-2, 3, 5, 6; H-7 → C-1, 6, 10, 21; H-8 → C-7, 9; H-9 → C-1, 8; H-10a → C-6, 7, 21; H-10b → C-6, 7, 21; H-11 → C-8, 9; H-12 → C-1, 8, 9; H-13 → C-1, 2, 3; H-20a → C-14, 19, 21; H-20b → C-14, 19, 21; H-22 → C-10, 14, 19, 21, 23; H-23 → C-14, 21, 22; H-24 → C-14, 15, 16; H-25 → C-16, 17, 18; OH-3 → C-2, 3, 4; OH-16 → C-15, 16, 17; OH-18 → C-18, 19; HRESIMS *m/z* 425.1973 (calcd. for C<sub>25</sub>H<sub>29</sub>O<sub>6</sub>, 425.1969).

**Spirocitrinol B (2):** colorless oil; [α]<sup>25</sup><sub>D</sub> -16.6 (c 0.1, MeOH); UV (MeOH)  $\lambda_{\text{max}}$  (log ε) 205 (0.40), 281 (0.08); IR (KBr)  $\nu_{\text{max}}$  3421, 2931, 1606, 1105, 964 cm<sup>-1</sup>; ECD (c 1.2 × 10<sup>-4</sup> M, MeOH)  $\lambda_{\text{max}}$  (Δε) 212 (-13.15), 278 (-0.65) nm; <sup>1</sup>H and <sup>13</sup>C NMR data see Table 1; HMBC data (DMSO-*d*<sub>6</sub>, 600 MHz) H-7 → C-1, 6; H-8 → C-7, 9; H-9 → C-1, 8; H-10a → C-7, 21; H-10b → C-7, 21; H-11 → C-8, 9; H-12 → C-1, 8, 9; H-13 → C-1, 2, 3; H-20a → C-14, 19, 21; H-20b → C-10, 14, 19, 21, 23; H-22 → C-10, 14, 19, 21, 23; H-23 → C-14, 21, 22; H-24 → C-14, 15, 16; H-25 → C-16, 17, 18; H-29 → C-27, 28, 30; H-32 → C-3, 4, 5, H-33 → C-32, 34; H-34 → C-26, 31, 33; H-35 → C-33, 34; H-36 → C-26, 33, 34; H-37 → C-26, 27, 28; OH-3 → C-2, 3; OH-30 → C-29, 30, 31; HRESI-MS *m/z* 631.2917 (calcd. for C<sub>37</sub>H<sub>43</sub>O<sub>9</sub>, 631.2912).

### Computational details<sup>10</sup>

Conformational analysis within an energy window of 3.0 kcal mol<sup>-1</sup> was performed by using the OPLS3 molecular mechanics force field via the MacroModel panel of Maestro 10. The conformers were then further optimized with the software package Gaussian 09 at the B3LYP/6-31G(d) level, and the harmonic vibrational frequencies were also calculated to confirm their stability. Then the 60 lowest electronic transitions



for the obtained conformers in vacuum were calculated using time-dependent density functional theory (TD-DFT) methods at the CAM-B3LYP/6-31G(d) level. ECD spectra of the conformers were simulated using a Gaussian function. The overall theoretical ECD spectra were obtained according to the Boltzmann weighting of each conformer.

### Cytotoxicity assays

MTT assays were performed as previously described.<sup>11,12</sup> Briefly, cells were seeded into 96-well plates at a density of  $5 \times 10^3$  cells per well for 24 h, and were exposed to different concentrations of test compounds. After incubation for 72 h, cells were stained with 25  $\mu\text{L}$  of MTT solution (5 mg  $\text{mL}^{-1}$ ) for 25 min. Finally, the mixture of medium and MTT solution was removed and 75  $\mu\text{L}$  DMSO was added to dissolve formazan crystals. Absorbance of each well was measured at 544 nm (test wavelength) and 690 nm (background) using the Multi-Mode Microplate Reader. Background was subtracted from the absorbance of each well. A549 (human lung cancer) and Huh7 (human hepatoma), and HepG2 (human hepatoma) was purchased from the American Type Culture Collection (ATCC). SK-BR-3 (human breast cancer) was purchased from the Procell Life Science&Technology Co., Ltd J82 (human bladder cancer cell line) and MB49 (WT) (mouse bladder carcinoma cell line) was obtained from the Merck Millipore. MB49 (STR), the cisplatin resistant subclone of MB49 cells, was established in our lab by weekly exposure to cisplatin.

## Conclusions

In summary, spirocitrinols A (**1**) and B (**2**) are new citrinin derivatives with a spiro[chromane-2,3'-isochromane] skeleton. Compound **1** shares the same plane structure as the known fungal metabolites xerucitrinin A and B, but differs in having different configurations at C-7/C-21. Compound **2** possesses the same spiro[chromane-2,3'-isochromane] skeleton as **1**, but differs in having a 3,4,5-trimethylisochromane-6,8-diol unit at C-4 *via* C-C linkage between C-4 and C-32. Although citrinin dimers have been documented in many *P. citrinum* strains,<sup>2</sup> only three trimeric citrinin derivatives, tricitrinols A-C have been reported.<sup>3</sup> To our knowledge, spirocitrinol B (**2**) is the fourth example of trimeric citrinin metabolite, and is the first example possessing the spiro[chromane-2,3'-isochromane] skeleton. Dimeric and trimeric citrinin are described to be derived from the same or different citrinin monomers through Diels-Alder, Michael addition, or nucleophilic reactions.<sup>2,3</sup> Natural occurring citrinin-anthraquinone, and citrinin-alkaloid adducts also have been documented from *P. citrinum* strains.<sup>8h,i</sup> From a biosynthetic aspect, **1** and **2** could be derived from a hypothetical precursor **e**, which is formed *via* an intermolecular hetero Diels-Alder reaction between **c** and **d**.<sup>2a,6</sup> Although the known compounds **a** and **b** and the intermediates **c** and **d** were not coisolated in the current work, they could be the hypothetical biosynthetic precursors leading to the formation of **1** and **2** through a series of reactions including hetero Diels-Alder cycloaddition and Michael addition as illustrated in the

proposed plausible biosynthetic pathways shown in Scheme S1.<sup>2,3,13-16</sup>

## Conflicts of interest

The authors declare no conflict interest.

## Acknowledgements

This work was financially supported by the CAMS Innovation Fund for Medical Sciences (2021-1-I2M-030 and 2021-1-I2M-1-028).

## Notes and references

- (a) J. P. Brown, N. J. Cartwright, A. Robertson and W. B. Whalley, *Nature*, 1948, **162**, 72-73; (b) S. Kovac, P. Nemec and J. Balan, *Nature*, 1961, **190**, 1104-1105; (c) R. K. Hill and L. A. Gardella, *J. Org. Chem.*, 1964, **29**, 766-767.
- (a) D. Wakana, T. Hosoe, T. Itabashi, K. Okada, G. M. D. C. Takaki, T. Yaguchi, K. Fukushima and K. I. Kawai, *J. Nat. Med.*, 2006, **60**, 279-284; (b) Z. Y. Lu, Z. J. Lin, W. L. Wang, L. Du, T. J. Zhu, Y. C. Fang, Q. Q. Gu and W. M. Zhu, *J. Nat. Prod.*, 2008, **71**, 543-546; (c) L. Du, D. H. Li, G. J. Zhang, T. J. Zhu, J. Ai and Q. Q. Gu, *Tetrahedron*, 2010, **66**, 9286-9290; (d) W. Q. Guo, D. Li, J. X. Pen, T. J. Zhu, Q. Q. Gu and D. H. Li, *J. Nat. Prod.*, 2015, **78**, 306-310; (e) L. Chen, Y. Y. Zhao, R. F. Lan, L. Du, B. S. Wang, T. Zhou, Y. P. Li, Q. Q. Zhang, M. G. Ying, Q. H. Zheng and Q. Y. Liu, *Tetrahedron*, 2017, **73**, 5900-5911; (f) L. Wang, C. L. Li, G. H. Yu, Z. C. Sun, G. J. Zhang, Q. Q. Gu, T. J. Zhu, Q. Che, H. S. Guan and D. H. Li, *Tetrahedron Lett.*, 2019, **60**, 151182; (g) W. Y. Wang, Y. Y. Liao, B. B. Zhang, M. L. Gao, W. Q. Ke, F. Li and Z. Z. Shao, *Mar. Drugs*, 2019, **17**, 46; (h) A. Sabdaningsih, Y. Liu, U. Mettal, J. Heep, Riyanti, L. Wang, O. Cristianawati, H. Nuryadi, M. T. Sibero, M. Marner, O. K. Radjasa, A. Sabdono, A. Trianto and T. F. Schäberle, *Mar. Drugs*, 2020, **18**, 227; (i) H. T. Li, R. T. Duan, T. Liu, R. N. Yang, J. P. Wang, S. X. Liu, Y. B. Yang, H. Zhou and Z. T. Ding, *Fitoterapia*, 2020, **146**, 104711; (j) M. M. Cheng, P. L. Li, Y. Jiang, X. L. Tang, W. J. Zhang, Q. Wang and G. Q. Li, *J. Nat. Prod.*, 2021, **84**, 1345-1352; (k) H. Fan, Z. M. Shi, Y. H. Lei, M. X. Si-Tu, F. G. Zhou, C. Feng, X. Wei, X. H. Shao, Y. Chen and C. X. Zhang, *Mar. Drugs*, 2022, **20**, 443.
- (a) L. Du, H. C. Liu, W. Fu, D. H. Li, Q. M. Pan, T. J. Zhu, M. Y. Geng and Q. Q. Gu, *J. Med. Chem.*, 2011, **54**, 5796-5810; (b) J. H. Wei, X. X. Chen, Y. C. Ge, Q. Z. Yin, X. D. Wu, J. S. Tang, Z. J. Zhang and B. Wu, *J. Org. Chem.*, 2022, **87**, 13270-13279.
- J. M. Gao, S. X. Yang and J. C. Qin, *Chem. Rev.*, 2013, **113**, 4755-4811.
- (a) J. Sperry, Z. E. Wilson, D. C. K. Rathwell and M. A. Brimble, *Nat. Prod. Rep.*, 2010, **27**, 1117-1137; (b) D. J. Atkinson and M. A. Brimble, *Nat. Prod. Rep.*, 2015, **32**,



811–840; (c) K. Hiesinger, D. Dar'in, E. Proschak and M. Krasavin, *J. Med. Chem.*, 2021, **64**, 150–183.

6 K. Sadorn, S. Saepua, N. Boonyuen, P. Laksanacharoen, P. Rachtawee and P. Pittayakhajonwut, *RSC Adv.*, 2016, **6**, 94510–94523.

7 (a) L. Salendra, X. P. Lin, W. H. Chen, X. Y. Pang, X. W. Luo, J. Y. Long, S. R. Liao, J. F. Wang, X. F. Zhou, Y. H. Liu and B. Yang, *Nat. Prod. Res.*, 2021, **35**, 900–908; (b) S. J. Chen, D. M. Tian, J. H. Wei, C. Li, Y. H. Ma, X. S. Gou, Y. R. Shen, M. Chen, S. H. Zhang, J. Li, B. Wu and J. S. Tang, *Front. Mar. Sci.*, 2022, 961356.

8 (a) C. H. Chen, C. Y. Shaw, C. C. Chen and Y. C. Tsai, *J. Nat. Prod.*, 2002, **65**, 740–741; (b) T. Amagata, A. Amagata, K. Tenney, F. A. Valeriote, E. Lobkovsky, J. Clardy and P. Crews, *Org. Lett.*, 2003, **5**, 4393–4396; (c) M. Tsuda, Y. Kasai, K. Komatsu, T. Sone, M. Tanaka, Y. Mikami and J. Kobayashi, *Org. Lett.*, 2004, **6**, 3087–3089; (d) M. Tsuda, M. Sasaki, T. Mugishima, K. Komatsu, T. Sone, M. Tanaka, Y. Mikami and J. Kobayashi, *J. Nat. Prod.*, 2005, **68**, 273–276; (e) M. Sasaki, M. Tsuda, M. Sekiguchi, Y. Mikami and J. Kobayashi, *Org. Lett.*, 2005, **7**, 4261–4264; (f) T. Mugishima, M. Tsuda, Y. Kasai, H. Ishiyama, E. Fukushi, J. Kawabata, M. Watanabe, K. Akao and J. Kobayashi, *J. Org. Chem.*, 2005, **70**, 9430–9435; (g) L. Du, T. J. Zhu, Y. C. Fang, Q. Q. Gu and W. M. Zhu, *J. Nat. Prod.*, 2008, **71**, 1343–1351; (h) N. Khamthong, V. Rukachaisirikul, S. Phongpaichit, S. Preedanon and J. Sakayaroj, *Tetrahedron*, 2012, **68**, 8245–8250; (i) M. El-Neketi, W. Ebrahim, W. Lin, S. Gedara, F. Badria, H. E. A. Saad, D. Lai and P. Proksch, *J. Nat. Prod.*, 2013, **76**, 1099–1104; (j) K. Trisawan, V. Rukachaisirikul, K. Borwornwiriyapan, S. Phongpaichi and J. Sakayaroj, *Tetrahedron Lett.*, 2014, **55**, 1336–1338; (k) L. H. Meng, Y. Liu, X. M. Li, G. M. Xu, N. Y. Ji and B. G. Wang, *J. Nat. Prod.*, 2015, **78**, 2301–2305.

9 (a) L. Liu, Y. Li, S. Liu, Z. Zheng, X. Chen, H. Zhang, L. Guo and Y. Che, *Org. Lett.*, 2009, **11**, 2836–2839; (b) C. Ma, Y. Li, S. Niu, H. Zhang, X. Liu and Y. Che, *J. Nat. Prod.*, 2011, **74**, 32–37; (c) J. Ren, F. Zhang, X. Liu, L. Li, G. Liu, X. Liu and Y. Che, *Org. Lett.*, 2012, **14**, 6226–6229; (d) E. Li, F. Zhang, S. Niu, X. Liu, G. Liu and Y. Che, *Org. Lett.*, 2012, **14**, 3320–3323; (e) J. Zhang, L. Liu, B. Wang, Y. Zhang, L. Wang, X. Liu and Y. Che, *J. Nat. Prod.*, 2015, **78**, 3058–3066; (f) F. Ren, S. Chen, Y. Zhang, S. Zhu, J. Xiao, X. Liu, R. Su and Y. Che, *J. Nat. Prod.*, 2018, **81**, 1752–1759; (g) J. Zhang, Y. Li, F. Ren, Y. Zhang, X. Liu and Y. Che, *J. Nat. Prod.*, 2019, **82**, 1678–1685.

10 M. J. Frisch, G. W. Trucks, H. B. Schlegel, G. E. Scuseria, M. A. Robb, J. R. Cheeseman, G. Scalmani, V. Barone, B. Mennucci, G. A. Petersson, H. Nakatsuji, M. Caricato, X. Li, H. P. Hratchian, A. F. Izmaylov, J. Bloino, G. Zheng, J. L. Sonnenberg, M. Hada, M. Ehara, K. Toyota, R. Fukuda, J. Hasegawa, M. Ishida, T. Nakajima, Y. Honda, O. Kitao, H. Nakai, T. Vreven, J. A. Montgomery Jr, J. E. Peralta, F. Ogliaro, M. Bearpark, J. J. Heyd, E. Brothers, K. N. Kudin, V. N. Staroverov, R. Kobayashi, J. Normand, K. Raghavachari, A. Rendell, J. C. Burant, S. S. Iyengar, J. Tomasi, M. Cossi, N. Rega, J. M. Millam, M. Klene, J. E. Knox, J. B. Cross, V. Bakken, C. Adamo, J. Jaramillo, R. Gomperts, R. E. Stratmann, O. Yazyev, A. J. Austin, R. Cammi, C. Pomelli, J. W. Ochterski, R. L. Martin, K. Morokuma, V. G. Zakrzewski, G. A. Voth, P. Salvador, J. J. Dannenberg, S. Dapprich, A. D. Daniels, O. Farkas, J. B. Foresman, J. V. Ortiz, J. Cioslowski and D. J. Fox, *Gaussian 09, Rev D.01*, Gaussian, Inc., Wallingford, CT, 2009.

11 C. Y. Wang, L. Engelke, D. Bickel, A. Hamacher, M. Frank, P. Proksch, H. Gohlke and U. M. Kassack, *Bioorg. Med. Chem.*, 2019, **27**, 115044.

12 N. Zhang, Y. Chen, R. Jiang, E. Li, X. Chen, Z. Xi, Y. Guo, X. Liu, Y. Zhou, Y. Che and X. Jiang, *Autophagy*, 2011, **7**, 598–612.

13 (a) H. Hajjaj, A. Klaebe, M. O. Loret, G. Goma, P. J. Blanc and J. Francois, *Appl. Environ. Microbiol.*, 1999, **65**, 311–314; (b) B. R. Clark, R. J. Capon, E. Lacey, S. Tenant and J. H. Gill, *Org. Biomol. Chem.*, 2006, **4**, 1520–1528.

14 D. Zhang, X. Li, J. S. Kang, H. D. Choi, J. H. Jung and B. W. Son, *J. Microbiol. Biotechnol.*, 2007, **17**, 865–867.

15 Q. Chen, J. Gao, C. Jamieson, J. Liu, M. Ohashi, J. Bai, D. Yan, B. Liu, Y. Che, Y. Wang, K. N. Houk and Y. Hu, *J. Am. Chem. Soc.*, 2019, **141**, 14052–14056.

16 Y. Zhai, Y. Li, J. Zhang, Y. Zhang, F. Ren, X. Zhang, G. Liu, X. Liu and Y. Che, *Fungal Genet. Biol.*, 2019, **129**, 7–15.

